Communication

# Determination of the Crystal Structure of Substrate-Induced Pentacene Polymorphs in Fiber Structured Thin Films

Stefan Schiefer, Martin Huth, Alexander Dobrinevski, and Bert Nickel

*J. Am. Chem. Soc.*, **2007**, 129 (34), 10316-10317• DOI: 10.1021/ja0730516 • Publication Date (Web): 02 August 2007



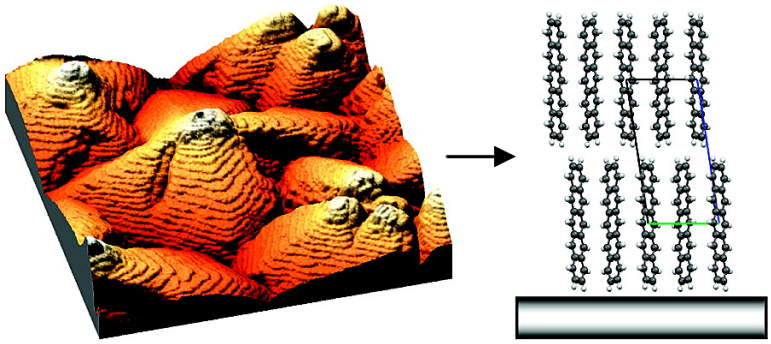

J|A|C|S
COMMUNICATIONS

Published on Web 08/02/2007

# Determination of the Crystal Structure of Substrate-Induced Pentacene Polymorphs in Fiber Structured Thin Films

Stefan Schiefer, Martin Huth, Alexander Dobrinevski, and Bert Nickel*

*Department für Physik and CeNS, Ludwig-Maximilians-Universität, Geschwister-Scholl-Platz 1, 80539 München, Germany*

Received May 1, 2007; E-mail: nickel@lmu.de

The intrinsic charge transport properties in organic crystals as calculated by numerical methods depend strongly on the molecular packing and arrangement in the crystal.[1−4] Pentacene, showing one of the highest charge carrier mobilities among organic semiconductors,[5,6] is known to crystallize in at least four polymorphs, which can be distinguished by their layer periodicity[7] $d_{(001)}$. Only two polymorphs grow as single crystals, and their crystal structure has been solved.[7,8] The substrate-induced 15.4 Å polymorph is the most relevant for organic thin-film transistor (OTFT) applications; however, its crystal structure has remained incomplete[7,9−13] as it only grows as a fiber structured thin film. Here we extend the crystal truncation rod X-ray scattering technique to fiber structured thin films. We determine the complete crystal structure of this polymorph grown on various substrates and find that the molecular arrangement within the unit cell is substrate dependent.

Pentacene crystallizes in a layered structure with a herringbone arrangement and grows at room temperature in the so-called "thin-film" phase on amorphous silicon dioxide[9] (a-$SiO_2$). Since X-ray reflectivity measurements only showed (00l) reflections associated with a spacing of $d_{(00l)} = 15.4$ Å, the crystallites are supposed to form a fiber structure with their $a-b$ plane oriented parallel to the substrate surface and the fiber axes parallel to the substrate normal[9] (Figure S1). The thin-film phase is a substrate-induced polymorph, as it is only observed near the substrate for film thicknesses of up to 50 nm at 300 K.[7,14] Hence, sample preparation for X-ray powder diffraction failed because insufficient sample could be produced,[7] and more importantly, it remains unclear if the thin-film phase can be removed from the substrate without changing its structure. The reciprocal unit cell parameters $a^*$, $b^*$, and $\gamma^*$ were obtained by electron diffraction experiments using electron transparent substrates such as thin copper grids coated with carbon.[8,15] Subsequent grazing incidence X-ray diffraction (GIXD) measurements on a-$SiO_2$ substrates revealed the in-plane unit cell parameters $a$, $b$ and their respective angle $\gamma$.[10−13] To solve the complete crystal structure, or the complete set of unit cell parameters and the molecular arrangement within the unit cell, a large reciprocal space section of Bragg peaks along with their intensities has to be measured and analyzed. Such a measurement has to overcome the inherently weak signal-to-noise ratio from the thin-film crystallites. Furthermore, a complex numerical analysis has to be developed to analyze the diffraction data of crystallites forming a fiber structure. Here we will employ a grazing incidence crystal truncation rod (GI-CTR)[16] geometry to cover the relevant section of reciprocal space for a substrate-supported thin film. Details of the experimental setup are given in the Supporting Information.

Here, we first focus on how to collect the relevant data set for pentacene thin films on technologically relevant substrates such as a-$SiO_2$, octadecyltrichlorosilane-treated a-$SiO_2$ (OTS), and Topas.[17] As a first step, the in-plane Bragg peak positions are determined by a GIXD measurement as described elsewhere.[10] For each in-plane Bragg peak, one GI-CTR scan is performed as follows: The incident X-ray beam is kept at a grazing angle $\alpha_i = 0.15°$ on the sample near the critical angle for total external reflection $\alpha_c$. The detector azimuth angle $\delta$ is set to $\delta'$, an in-plane Bragg peak position of interest. A scan is performed by measuring the diffracted intensity while increasing the altitude angle $\gamma$ and simultaneously adjusting $\delta$ by

$$\delta = \arcsin\left(\frac{2\cos(\delta')\cos(\alpha_i) + \cos^2(\gamma) - 1}{2\cos(\gamma)\cos(\alpha_i)}\right) \qquad (1)$$

This keeps the lateral momentum transfer $q_{xy}$ constant while the perpendicular momentum transfer $q_z$ is varied (Figure 1a). A highly collimated scintillating point detector is used for data collection, resulting in a Bragg signal with a signal-to-noise ratio of $\sim 10^3$. Background intensity is measured with an offset of $\Delta\delta = 1°$ and is subtracted.

Solving the crystal structure is achieved in a two-step procedure. First, the unit cell parameters are solved from those Bragg peak positions ($q_{xy}$, $q_z$) which can be assigned unambiguously to a Miller index.

After the unit cell parameters are determined, the molecular arrangement within the unit cell is inferred from the measured intensity distributions of all measured data points $I(q_{xy},q_z)$. Technically, this is realized by simulating the sum of all individual intensities $m$ superimposing due to the fiber structure (Figure 1b). For the simulation of the scattered GI-CTR intensity $I(q_{xy},q_z)$, we use the semi-kinematical approximation:

$$I(q_{xy},q_z) = C\cdot(A_0 N_A N_B)^2 \sum_m \left| e^{-B\cdot q_m^2}\cdot F(\vec{q}_m)\cdot \frac{e^{N_c(i\cdot\vec{q}_m\cdot\vec{c}-\sigma)} - 1}{e^{i\cdot\vec{q}_m\cdot\vec{c}-\sigma} - 1}\right|^2 \qquad (2)$$

where $A_0$ represents the incident intensity, $C$ includes beam amplitude correction factors,[18] $B$ is the B-factor of the Debye−Waller factor, $N_a N_b$ are the number of unit cells of a crystallite in $\vec{a}$ and $\vec{b}$ direction, $N_c$ is the film thickness in unit cells, and $\sigma$ is the surface roughness, which describes the observed surface morphology of a pentacene thin-film crystallite.

The structure factor $F(\vec{q}_m)$ is calculated from a unit cell consisting of two pentacene molecules arranged in a herringbone structure. The positions of the molecules are fixed with their center of mass at the unit-cell coordinates (0, 0, 0) for molecule A and ($^1/_2$, $^1/_2$, 0) for molecule B. The structure of the pentacene molecule was taken from the 14.1 Å crystal structure,[8] and the Cromer−Mann scattering factor coefficients were used. The three angular degrees of freedom of each molecule were fitted independently. The angle between the two molecular planes is called the herringbone angle $\theta_{hrgb}$ as illustrated in Figure 2a. The tilt angle of the long molecular axis (LMA, Figure 2b) with respect to the


10.1021/ja0730516 CCC: $37.00 

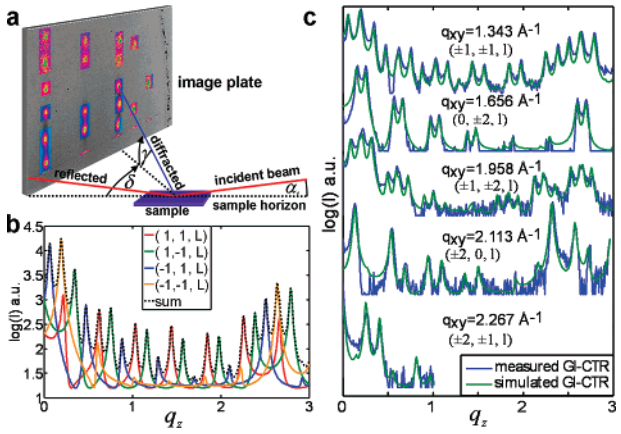


***Figure 1.*** (a) GI-CTR geometry. Note that the sample does not move during a measurement. Here, the point detector is replaced by an image plate for better illustration. (b) Simulation of the $h = k = \pm 1$ GI-CTR contributions and their superposition (dotted line). (c) Observed and best fit plots of GI-CTRs of the 15.4 Å pentacene thin-film phase on a-$SiO_2$.

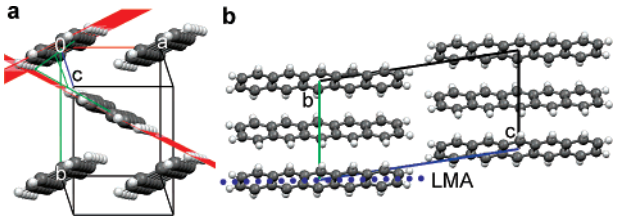


***Figure 2.*** Three-dimensional view of 15.4 Å pentacene thin-film polymorph on $SiO_2$. (a) Top view: the herringbone angle between the two red molecule planes is illustrated in green. (b) Side view: the LMA is illustrated as a dotted line.

substrate surface normal is called $\varphi_A$ for molecule A and $\varphi_B$ for molecule B. With model simulations using eq 2, we verified that GI-CTR measurements with a signal-to-noise ratio $\geq 10^3$ are needed to detect the weak Bragg peaks which are most sensitive to the molecular arrangement, such as a variation of the herringbone angle. The measurements for the a-$SiO_2$ substrate and the best fits are plotted in Figure 1c. Notice that the used model reproduces the whole line shape of the measurements well. Forty-seven Bragg peak positions could be clearly assigned to a Miller index and were used to solve the unit cell parameters. We found that the unit cell parameters are identical within measurement precision on all measured substrates. The crystal structure was found to be triclinic with the following lattice parameters: $a = 5.958 \pm 0.005$ Å, $b = 7.596 \pm 0.008$ Å, $c = 15.61 \pm 0.01$ Å, $\alpha = 81.25 \pm 0.04°$, $\beta = 86.56 \pm 0.04°$, and $\gamma = 89.80 \pm 0.10°$. The unit cell volume $V = 697$ Å$^3$ is the largest of all pentacene polymorphs reported so far; $a$, $b$, and $\gamma$ differ only slightly from values reported from previous GIXD studies.[10−13] The unit cell angles $\alpha$, $\beta$, and $\gamma$ are in close correspondence to the values recently reported by Yoshida,[19] although the unit cell axes $a$, $b$, and $c$ differ slightly. Here, we find a herringbone angle $\theta_{hrgb}$ of 54.3, 55.8, and 59.4° for a-$SiO_2$, OTS, and Topas, respectively. The tilts of the two molecular axes ($\varphi_A$, $\varphi_B$) are (5.6°, 6.0°), (6.4°,6.8°), and (5.6°, 6.3°) for a-$SiO_2$, OTS, and Topas, respectively.

To conclude, we showed that the molecular orientation in the unit cell differs among different substrates while the unit cell dimensions of the 15.4 Å pentacene polymorph are identical. This indicates that substrate effects have to be included if one aims to understand the molecular structure of the thin-film phase[19] in detail.

The crystal structures reported here (atomic coordinates are given in the Supporting Information as cif files) provide a basis to apply techniques such as density functional methods to investigate intrinsic charge transport properties[1,2] and optical properties of organic thin-film devices on a molecular level. In previous studies, it was observed that different substrates vary the charge carrier mobility in OTFTs.[20] The substrate-dependent crystal structures observed here could be one reason for this variation. This topic may lead ultimately to a controlled fine-tuning of intrinsic charge transport properties.

The experimental approach to determine the crystal structure developed here can be easily applied to a wide range of organic thin-film systems used in organic electronic devices.

**Acknowledgment.** We acknowledge support and helpful discussions with O.H. Seeck, J. Pflaum, W. Schmahl, J.O. Rädler, M. Fiebig, S. Youssef, and N. Tsao, and financial support from HASYLab, Hamburg, DFG Schwerpunkt 1121 and CeNS. S.S. acknowledges a scholarship from the Elite Network of Bavaria.

**Supporting Information Available:** Sample preparation, AFM images, X-ray diffractometer setup, X-ray analysis, .cif files. This material is available free of charge via the Internet at http://pubs.acs.org.

## References

(1) Troisi, A.; Orlandi, G. *J. Phys. Chem. B* **2005**, *109*, 1849−1856.
(2) Troisi, A.; Orlandi, G. *Phys. Rev. Lett.* **2006**, *96*, 4.
(3) Cornil, J.; Calbert, J. P.; Bredas, J. L. *J. Am. Chem. Soc.* **2001**, *123*, 1250−1251.
(4) Cheng, Y. C.; Silbey, R. J.; da Silva, D. A.; Calbert, J. P.; Cornil, J.; Bredas, J. L. *J. Chem. Phys.* **2003**, *118*, 3764−3774.
(5) Lin, Y. Y.; Gundlach, D. J.; Nelson, S. F.; Jackson, T. N. *IEEE Electron Device Lett.* **1997**, *18*, 606−608.
(6) Kelley, T. W.; Baude, P. F.; Gerlach, C.; Ender, D. E.; Muyres, D.; Haase, M. A.; Vogel, D. E.; Theiss, S. D. *Chem. Mater.* **2004**, *16*, 4413−4422.
(7) Mattheus, C. C.; Dros, A. B.; Baas, J.; Oostergetel, G. T.; Meetsma, A.; de Boer, J. L.; Palstra, T. T. M. *Synth. Met.* **2003**, *138*, 475−481.
(8) Mattheus, C. C.; Dros, A. B.; Baas, J.; Meetsma, A.; de Boer, J. L.; Palstra, T. T. M. *Acta Crystallogr., Sect. C* **2001**, *57*, 939−941.
(9) Dimitrakopoulos, C. D.; Brown, A. R.; Pomp, A. *J. Appl. Phys.* **1996**, *80*, 2501−2508.
(10) Ruiz, R.; Mayer, A. C.; Malliaras, G. G.; Nickel, B.; Scoles, G.; Kazimirov, A.; Kim, H.; Headrick, R. L.; Islam, Z. *Appl. Phys. Lett.* **2004**, *85*, 4926−4928.
(11) Fritz, S. E.; Martin, S. M.; Frisbie, C. D.; Ward, M. D.; Toney, M. F. *J. Am. Chem. Soc.* **2004**, *126*, 4084−4085.
(12) Yang, H. C.; Shin, T. J.; Ling, M. M.; Cho, K.; Ryu, C. Y.; Bao, Z. N. *J. Am. Chem. Soc.* **2005**, *127*, 11542−11543.
(13) Drummy, L. F.; Martin, D. C. *Adv. Mater.* **2005**, *17*, 903.
(14) Mayer, A. C.; Kazimirov, A.; Malliaras, G. G. *Phys. Rev. Lett.* **2006**, *97*, 4.
(15) Wu, J. S.; Spence, J. C. H. *J. Appl. Crystallogr.* **2004**, *37*, 78−81.
(16) Feidenhansl, R. *Surf. Sci. Rep.* **1989**, *10*, 105−188.
(17) Topas is the trade name for Ticona cyclo-olefin copolymers (COC), a flexible and optical transparent substrate.
(18) Smilgies, D. M. *Rev. Sci. Instrum.* **2002**, *73*, 1706−1710.
(19) Yoshida, H.; Katsuhiko, I.; Sato, N. *Appl. Phys. Lett.* **2007**, *90*, 181930.
(20) Shtein, M.; Mapel, J.; Benziger, J. B.; Forrest, S. R. *Appl. Phys. Lett.* **2002**, *81*, 268−270.

JA0730516